Journal of Applied Physics ARTICLE scitation.org/journal/jap

The effect of vacancy-impurity complexes in silicon on the current–voltage characteristics of p–n junctions

Cite as: J. Appl. Phys. **128**, 155702 (2020); doi: 10.1063/5.0023411
Submitted: 29 July 2020 · Accepted: 2 October 2020 ·
Published Online: 15 October 2020

Sergey V. Bulyarskiy,[1,a)] Alexander V. Lakalin,[1] Mikhail A. Saurov,[2] and Georgy G. Gusarov[1]

AFFILIATIONS

[1]Institute of Nanotechnology of Microelectronics of the Russian Academy of Sciences (INME RAS), Leninskiy prospect, 32A, Moscow 119991, Russia
[2]National Research University of Electronic Technology (MIET), Zelenograd, Moscow 124498, Russia

[a)]**Author to whom correspondence should be addressed:** bulyar2954@mail.ru

ABSTRACT

The methods for analyzing the current–voltage characteristics of p–n junctions at forward and reverse bias with the calculation of the parameters of recombination centers before and after irradiation with gamma quanta were developed in this work. These methods are simple, convenient, and allow one to determine the parameters of deep levels at one temperature, which makes it possible to use them as express diagnostic techniques, taking measurements immediately on the semiconductor plates at the completion of the main technological processes. It was shown that after irradiation the composition of the centers in the depletion region of the p–n junction changes, the recombination processes and the lifetime begin to determine the divacancy complexes of silicon with oxygen (V_2O). It was found that the generation of charge carriers in a strong field of the depletion region of the p–n junction occurs under the influence of the electron–phonon interaction, the parameters of this interaction are determined, and the configuration-coordinate diagrams of recombination centers are constructed.

I. INTRODUCTION

An interest to the studies of defects is connected with their obvious and important influence on the structurally sensitive characteristics and the kinetics of photo- and other processes in semiconductors, especially on the generation–recombination processes in p–n junctions.[1] Czochralski (CZ) silicon is a dominating material for current photovoltaic and microelectronic industry. This semiconductor contains a wide variety of defects that should be studied. In Ref. 2, a very detailed analysis of complexes in silicon was made, including vacancy–impurity complexes. Oxygen is an important impurity located at interstitial sites in the silicon lattice, with a concentration of $\sim 10^{18}\,cm^{-3}$ in CZ silicon. Vacancies are easily trapped by oxygen atoms, leading to a formation of vacancy-oxygen (VO) complexes. Upon annealing, VO complex can combine with vacancy or interstitial oxygen to form more complicated complexes, such as V_2O, VO_2, VO_3, and so on.[2] The study of silicon irradiation defects leads to a good understanding of the nature of secondary defects in silicon. Complexes prevail among them.[3–5] The formation of complexes in silicon leads to an increase in recombination currents and an increase in the reverse currents of silicon devices in the dark, which is associated with accelerated generation with the participation of complexes.[1,6–8]

Vacancies in silicon are easily captured by oxygen and form vacancy –oxygen complexes. Such complexes may contain a different number of both vacancies and oxygen. The complex of one vacancy with one oxygen atom (VO) is called the A-center; it creates an acceptor level in the bandgap of silicon with an energy measured from the conduction band, E_C–0.17 eV.[2] However, it is multicharged and amphoteric, since it has a donor level, whose energy is 0.76 eV from the conduction band.[9] The silicon vacancy in this complex has four equivalent positions and can be rearranged from one position to another with energy of 0.37 eV.[2] It affects the lifetime of minority charge carriers in silicon.

The VO_2 complexes in silicon are observed by various methods, including infrared absorption, where they create bands of

887 and 895 cm^{-1},[2,10] and by the method of studying electrical properties,[11] where this complex appears as a level with an energy of 0.16–0.19 eV. Under radiation exposure, divacancy[10,12,13] and the V_2O complex[13–15] are often formed, which is associated with an increase in the concentration of vacancies during irradiation. Divacancy is a multiply charged center in silicon and creates several energy levels. Measurements by deep level transient spectroscopy (DLTS) show the presence of levels 0.23 and 0.3 eV,[11,12] as well as 0.25 and 0.44 eV.[14] The energy levels, which are associated with the V_2O center, have energies of 0.23 and 0.45 eV, which are close to divacancy energies. As part of the processes of secondary defect formation, a reaction of the conversion of the A-center to the V_2O center is observed,[9,15–18]

$$VO + V = V_2O.$$

Table I of parameters of the levels of complexes associated with oxygen and vacancies in silicon summarizes the results by different researchers presented above.

An important task is the rapid diagnosis of defects by current–voltage characteristics (CVCs), which can be measured on silicon wafers, even before cutting them into separate devices. These characteristics contain important information about defects;[1,20–23] nevertheless, one needs to be able to correctly extract them from experiment. The fundamental principles of the theory of recombination generation in semiconductor diodes were laid in classical works.[24,25] However, the opportunities that are inherent in them are not being used properly. There are important works in which the recombination currents of p–n junctions were analyzed.[26–29] These works develop methods for analyzing recombination processes and conditions for the applicability of one or another model CVC under forward bias; however, the simplified Shockley model is often used when the electron and hole capture cross sections for the recombination center (RC) are considered the same. This approach is not true. A change in the ratio of the capture cross sections leads to a change in the injection level at which the center is recharged and this affects the features of the CVC. This effect becomes especially pronounced when CVC are transformed according to certain algorithms and their differential parameters are studied.[21–23]

There are drawbacks to the analysis of p–n junction currents with reverse bias. From the point of view of the ideal diode diffusion theory of the flow of the p–n junction current, the reverse current should not depend on the applied voltage.[24] Its growth upon irradiation of the device is associated with a change in the lifetime during irradiation.[30] The activation energy of the temperature dependence of the ideal diode diffusion current should be equal to the energy of the semiconductor bandgap; however, experimental studies show that this is not so and the energy is less than the bandgap width.[1,31] This is due to the fact that in most cases, the reverse current is the sum of the diffusion current and the generation current,[25] with the latter prevailing.[1] The mechanism of current flow can be determined by studying its dependence on temperature. If the experimental value of the activation energy of the current is less than the energy of the bandgap, but more than half, then the reverse current is determined by the process of generation of electrons and holes through the levels of deep centers and should not depend on the bias voltage at the p–n junction. The generation of electrons and holes occurs in the space charge region (SCR) of the p–n junction, where there is a sufficiently strong electric field that affects the magnitude of the current. In most studies that investigate the reverse CVC of semiconductor devices, this phenomenon is ignored, while in others the influence of the applied voltage is explained by the Poole–Frenkel effect.[32,33] The Poole–Frenkel coefficient has a clearly defined theoretical value. This value must be calculated and compared with its experimental value in order to prove the existence of this effect. However, the Poole–Frenkel coefficient value calculated from the experimental results can be greater than the theoretical one, which is associated with the influence of electron–phonon interaction.[1,34] This influence can be quite strong in some cases, for example, the experimental reverse current of silicon thyristors[35] initially monotonically increases with increasing applied voltage and then becomes exponential. Without taking into account the electron–phonon interaction, this dependence cannot be explained.

In the present work, a detailed analysis of the recombination and generation currents in the SCR of semiconductor p–n junctions is carried out, and the conditions when these currents prevail are specified. Algorithms are developed for converting the CVC, their separation into recombination processes through various centers, and determining the parameters of the recombination

TABLE I. The parameters of vacancy-oxygen complexes in silicon from our literature survey.

Complex designation	Nature of transition	Activation energy (eV)	Capture cross section (cm^2)	Reference
A (VO)	$VO^- \rightarrow VO^0 + e$	0.167	4×10^{-16}	2, 14
V_2	$V_2^{-2} \rightarrow V_2^{-1} + e$	0.23–0.25	5×10^{-15}	2, 11–14
V_2	$V_2^{-1} \rightarrow V_2^{0} + e$	0.436	3×10^{-15}	14
V_2O	$V_2O^{-2} \rightarrow V_2O^{-1} + e$	0.24	3×10^{-16}	2, 11, 14
V_2O	$V_2O^{-1} \rightarrow V_2O^{0} + e$	0.454	7×10^{-15}	14
A5	?	0.33	2×10^{-15}	14
A (VO)	$VO^0 \rightarrow VO^{+-}e$	0.56	…	13
A (VO)	$VO^- \rightarrow VO^{+2-}e$	0.61	…	13
VO_2	…	0.35	…	2
E_5 (V_3)	…	0.39, 0.45	…	19

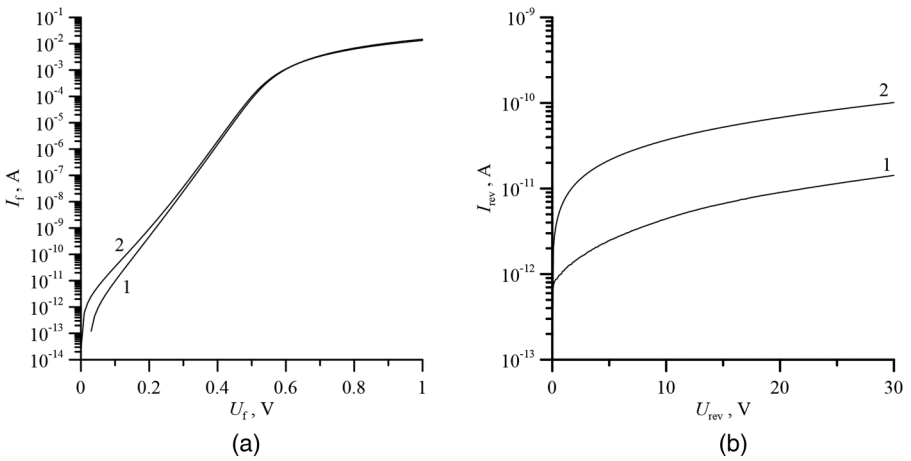

FIG. 1. Forward (a) and reverse (b) current–voltage characteristics at room temperature before (1) and after (2) irradiation.

centers, which contribute to the formation of the CVC, with the electron–phonon interaction being taken into account. The CVC of p–n junctions before and after irradiation with γ rays of the ^{60}Co isotope are studied. This example provides a methodology for processing such CVC, determines the parameters of the electron–phonon interaction, and constructs the coordinate diagrams of recombination centers, which demonstrate that a recombination center with a deep level in the bandgap of a semiconductor is not sufficient to characterize the energy of this level, but exists in the set of related parameters for this characteristic and these ones can be calculated from experiments. The work demonstrates algorithms and examples of these calculations.

II. EXPERIMENTAL RESULTS

Silicon photodiodes made on the basis of low-doped n-type silicon with a specific resistance of about 500 Ω cm were experimentally studied. The electrical characteristics of the diodes were measured, then they were irradiated, and these measurements were repeated again. The samples were irradiated with γ-quanta, which were emitted by a ^{60}Co-based source (γ-ray energy E ≈ 1.25 MeV). The radiation dose was 0.5 Mrad. Measurements were made of the CVC (I–V) of silicon photodiodes in the temperature range −30 to +60 °C both before and after irradiation. To measure the I–V characteristics, we used the B1500A semiconductor analyzer, which is optimized for measuring low-current signals up to 10^{-15} A and is equipped with special shielded triaxial terminals with a function for compensating ultra-low currents. The input resistance of the device (more than 100 TΩ) provides the most minimal level of introduced distortions and errors in the tested circuits in this class of devices during measurements.

Forward and reverse CVC before and after irradiation are shown in Fig. 1.

In the initial section of the CVC with forward bias, an increase in current was observed after irradiation. Since the current in this region is due to recombination in the SCR, we can conclude that the concentration of recombination centers increases. Reverse current also increased. The current through the diode at the reverse bias is due to the generation in the SCR and is proportional to the concentration of recombination centers. The generation current after irradiation increased 10 times. It can be assumed that the concentration of recombination centers increased 10 times after irradiation.

Reverse CVC plotted in coordinates $\ln(I) = f(F^{1/2})$ (where F is the electric field strength in the SCR of the diode) are linear (see Fig. 2). These facts indicate that the current through the diode at the reverse bias is caused by generation, and the Pool–Frenkel effect takes place, which lowers the height of the generation barrier in proportion to the root of the electric field strength.[1]

The temperature dependences of the reverse current plotted in the Arrhenius coordinates for various reverse bias voltages on the diode (see Fig. 3) allow us to determine the generation energies of charge carriers at various electric field strengths in the SCR of the

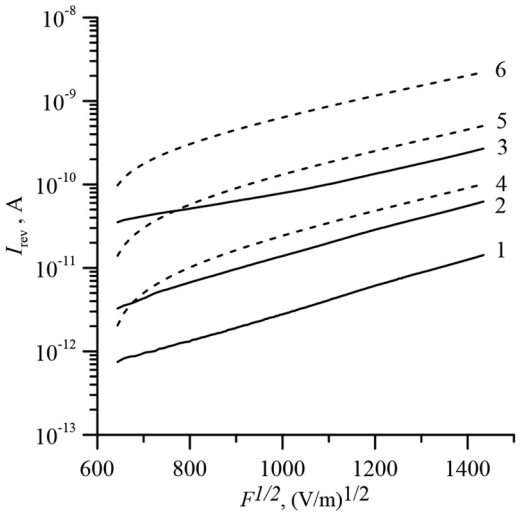

FIG. 2. CVC plotted in Poole–Frenkel coordinates before irradiation (1–3) and after irradiation (4–6) measured at temperatures (°C): 1.4–0; 2.5– 20; 3.6–40.

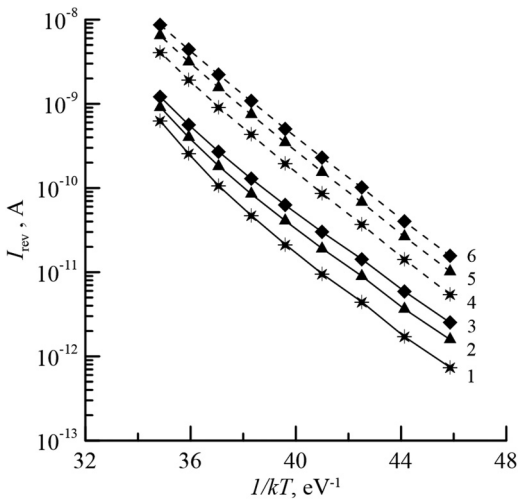

FIG. 3. Temperature dependences of the reverse current before irradiation (1–3), and after (4–5) at voltages, V: 1.4–10; 2.5–20; 3.6–30.

p–n junction. We must pay attention to the fact that the energies that are calculated from the Arrhenius dependences correspond to 0 K. These energies, which were calculated from the slope of the experimental CVC (see Fig. 3), depend on the electric field (see Fig. 4), which is also a manifestation of the Poole–Frenkel effect.

The experimental data presented show that the generation and recombination processes involving recombination centers determine the magnitude of the forward and reverse currents of the diodes. We will determine the parameters of these centers from the CVC.

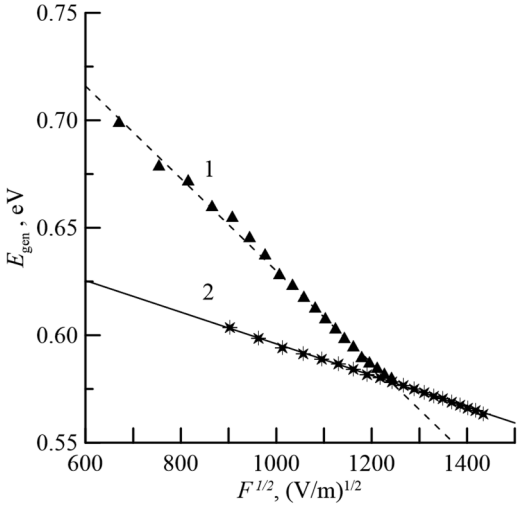

FIG. 4. Change in the activation energy of the generation process depending on the electric field: 1—before irradiation; 2—after irradiation.

III. DETERMINATION OF THE RECOMBINATION CENTERS PARAMETERS FROM CVC AT FORWARD BIAS

A. CVC of the diode at forward bias: Differential slope of the curve

The diode current when the forward bias voltage is applied is generated by several mechanisms. First of all, this is a diffusion current, the CVC of which is determined by the fundamental Shockley model,[24]

$$I = I_s\left(\exp\left(\frac{qU}{kT}\right) - 1\right), \quad I_s = qA\left(\frac{D_p p_{n0}}{L_p} + \frac{D_n n_{p0}}{L_n}\right), \tag{1}$$

where q is the elementary charge; k is the Boltzmann constant; A is the area of the p–n junction; U is the voltage ($U>0$ for forward bias, $U<0$ for reverse bias); I is the p–n junction current; T is the absolute temperature; p_{n0} and n_{p0} are the minority carrier concentrations; and D_n and D_p are diffusion coefficients of electrons and holes, which are linked with the magnitude of the charge carriers mobility by the Einstein relation: $D_n = kT\mu_n/q$, $D_p = kT\mu_p/q$. μ_n, where μ_p are the mobilities of electrons and holes. The diffusion coefficients are also related to the diffusion length: $L_n = \sqrt{D_n\,\tau_n}$, $L_p = \sqrt{D_p\,\tau_p}$. τ_n, where τ_p are the lifetimes of minority charge carriers.

It follows from this expression that the forward and reverse currents increase when the lifetime decreases, and the reverse current does not depend on voltage; it increases rapidly when the temperature increases. The activation energy of current growth in this case is equal to the bandgap.

The CVC during recombination in the SCR was obtained in Ref. 25 and can be represented as

$$I = \frac{qAw(U)n_i}{2\tau}\left(\exp\left(\frac{qU}{2kT}\right) - 1\right), \tag{2}$$

where $w(U)$ is the width of the SCR of the p–n junction; n_i is a concentration of intrinsic charge carriers; and τ is the lifetime of non-equilibrium charge carriers. The differential slope in this case is 2. Such an expression for recombination in the SCR was obtained under the simplifying assumption that the capture coefficients at the recombination center are equal for electrons and holes.

Formulas for the recombination current under forward bias without assuming equal capture coefficients were obtained in Refs. 1 and 20–23. In this case, the CVC during recombination through the center, which has one deep level in the bandgap of the semiconductor, has the form,

$$I_r(U) = \frac{qAw(U)\,c_n c_p n_i^2 N_t\left(\exp\left(\frac{qU}{kT}\right) - 1\right)}{2n_i\sqrt{c_n c_p}\exp\left(\frac{qU}{2kT}\right) + c_n n_1 + c_p p_1} \times \frac{2kT}{q(V_d - U)}, \tag{3}$$

where N_t is the concentration of recombination centers; V_d is the diffusion potential of the p–n junction; c_n and c_p are capture coefficients onto recombination centers; $n_1 = \gamma_n N_c \exp(-(E_C - E_t)/kT)$,

$p_1 = \gamma_p N_v \exp(-(E_t - E_V)/kT)$, and γ_n and γ_p are the degeneration factors of the deep center level for electrons and holes. These factors vary from 0.5 to 2.

The resulting current is equal to the sum of the recombination currents through each center, if several recombination centers are in the p–n junction,

$$I_r = \sum_{m=1}^{g} \frac{qAw(U)\, c_{nm} c_{pm} n_i^2 N_{tm} \left(\exp\left(\frac{qU}{kT}\right) - 1 \right)}{2n_i \sqrt{c_{nm} c_{pm}} \exp\left(\frac{qU}{2kT}\right) + c_{nm} n_{1m} + c_{pm} p_{1m}} \times \frac{2kT}{q(V_d - U)}, \tag{4}$$

where g is the number of doubly charged recombination centers simultaneously participating in the recombination process.

Formulas (3) and (4) lead to the value of the differential slope, which varies non-monotonically from 1 to 2.

The applicability criteria for formulas (3) and (4) were also obtained in Refs. 1 and 20–23. These criteria differ for different ratios of impurities in the n- and p-regions of the p–n junction. The diodes that are studied in this work are made on the basis of n-silicon with a low concentration of charge carriers by boron diffusion. In this case, the p–n junction is sharp and its p-region is doped more strongly than the n-region. The concentration of charge carriers in the n-region can be calculated from the capacitance–voltage characteristics shown in Fig. 5.

On the capacitance–voltage characteristics of the samples, there is a section within which the capacitance varies according to the law $C^{-2} = aU$, where a is a linear dependence coefficient. In our case, this section covers the entire region of reverse biases, which allows us to calculate the concentration of free charge carriers in the sample. This concentration before irradiation according to the results of measurements of several samples is $(5.9 \pm 0.2) \times 10^{11}$ cm^{-3}. As expected, the concentration of carriers is close to the concentration of intrinsic charge carriers. The concentration of free carriers after irradiation is $(5.5 \pm 0.2) \times 10^{11}$ cm^{-3}. Thus, the concentration after irradiation decreases. This is due to compensation effects in the samples as a result of the appearance of defects with deep levels that are caused by irradiation.

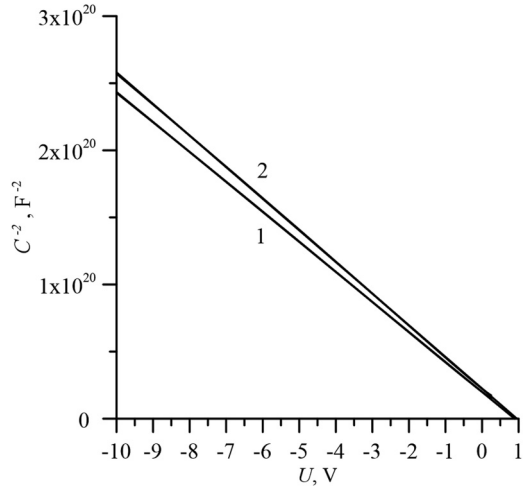

FIG. 5. Capacitance–voltage characteristics at room temperature in coordinates $C^{-2} = f(U)$: 1—before irradiation; 2—after irradiation.

In both cases, the n-region of the diodes is doped less than the p-region. In this case, the boundary voltage for the recombination region in the SCR is determined by the formula,[1]

$$U = V_d + \frac{kT}{q} \ln \frac{c_n n_n}{c_p p_p}, \tag{5}$$

where n_n is the concentration of free electrons in the n-region and p_p is the concentration of free holes in the p-region. The concentration of holes in the p-region is approximately 10^{17} cm^{-3}, as found from an estimate of the diffusion profiles; then, if we assume that the capture coefficients of electrons and holes are equal, the boundary voltage is less than the diffusion potential, which in this case is 0.6 V. Therefore, the region where recombination in the SCR occurs is lying at a voltage less than this value.

The current flow mechanism in forward bias, which is described by formulas (1)–(3), can be distinguished by the differential slope (β), which is different in these cases: for (1) $\beta = 1$; for (2) $\beta = 2$; and for (3) $1 < \beta < 2$. This indicator can be calculated from the experimental forward CVC by the formula,

$$\beta = \frac{qI}{kT} \left(\frac{dI}{dU} \right)^{-1} = \frac{q}{kT} \left(\frac{d \ln I}{dU} \right)^{-1}. \tag{6}$$

The calculation results of β for the diodes that were studied are shown in Fig. 6.

The experimental results of Fig. 6 show that the values of the differential slope are in the range $1 < \beta < 2$. The value of β exceeds 1 after irradiation more significantly. According to the results of Refs. 20 and 21, the presence of maxima in the dependence of the differential slope on the forward bias voltage indicates the existence of recombination centers. The differential slope shows two maxima (see Fig. 6), the first of which is blurred, which may be due to the influence of several recombination centers. These facts indicate that the direct CVC is determined by recombination in the SCR, and for processing the experimental CVC, we can use formulas (3) and (4).

B. Conversion of CVCs with forward bias

The experimental CVC underwent a transformation, which made it possible to better reveal their features. The dependence of a certain quantity on the forward bias voltage was calculated, which was called the reduced recombination rate ($R_{np}(U)$). This value is the inverse of the lifetime and has features that are associated with the parameters of recombination centers. The reduced

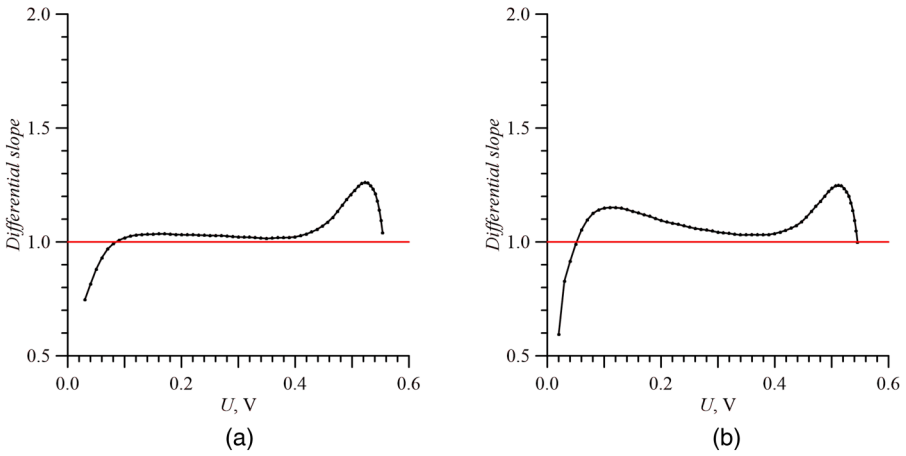

FIG. 6. Differential slope of the forward CVC of the diodes at room temperature: (a) before irradiation; (b) after irradiation.

recombination rate is defined as[22]

$$R_{np}(U) = \frac{I(U)\exp\left(\frac{qU}{2kT}\right)}{Aw(U)n_i\left(\exp\left(\frac{qU}{kT}\right)-1\right)} \times \frac{V_d(U)-U}{2kT}. \quad (7)$$

The validity range of this formula is $0 < U < V_d$.

Figure 7 shows the calculated reduced recombination rates of one of the samples at a temperature of 0 °C before and after irradiation.

The reduced recombination rate increases significantly in the low voltage region, which is associated with the creation of recombination centers. Its relationship with the parameters of these centers has the form,[22,23]

$$R_{np}(U) = \sum_{m=1}^{g} \frac{c_{nm}c_{pm}N_{tm}n_i\exp\left(\frac{qU}{2kT}\right)}{2n_i\sqrt{c_{nm}c_{pm}}\exp\left(\frac{qU}{2kT}\right)+c_{nm}n_{1m}+c_{pm}p_{1m}}, \quad (8)$$

where m is the number of the recombination center, c_n and c_p are the capture coefficients of electrons and holes by recombination centers, n_1, p_1 are the concentrations of free electrons and holes, respectively, when the Fermi level coincides with the level of the recombination center.

The function graph of the reduced recombination rate can be divided into two areas:

1. If $2n_i\sqrt{c_nc_p}\exp\left(\frac{qU}{2kT}\right) \ll (c_nn_1 + c_pp_1)$, then

$$R_{np} = \frac{c_nc_pn_iN_t\exp\left(\frac{qU}{2kT}\right)}{(c_nn_1+c_pp_1)}. \quad (9)$$

2. If $2n_i\sqrt{c_nc_p}\exp\left(\frac{qU}{2kT}\right) \gg (c_nn_1 + c_pp_1)$, then

$$R_{np} = \frac{\sqrt{c_nc_p}N_t}{2}. \quad (10)$$

In the first region, the function grows according to law (9); in the second, it is constant (10). We can single out the voltage U_{inf}, where the approximations of these two regions intersect. This voltage makes it possible to estimate the activation energy of the recombination center and then calculate the recombination parameters. In order to calculate this value, we equate formulas (9) and (10). In addition, it can almost always be considered that the recombination level is closer to one of the free zones. We assume that it is closer to the conduction band, then $c_nn_1 >> c_pp_1$ and we

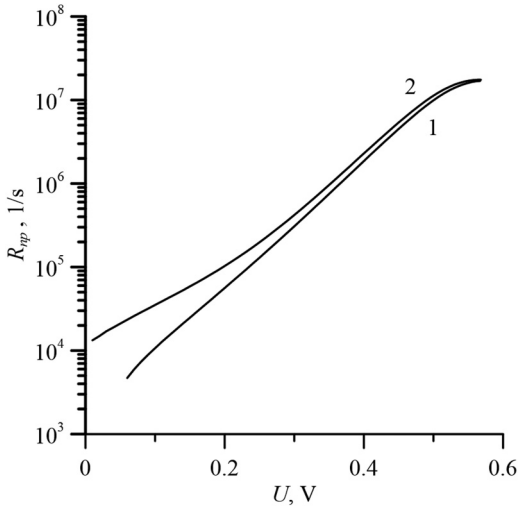

FIG. 7. The reduced recombination rate at a temperature of 0 °C: 1—before irradiation, 2—after irradiation.

obtain a formula that relates the activation energy of the recombination center E_t and U_{inf},

$$E_{tn} = \frac{E_g - qU_{\text{inf}}}{2} - kT \ln\left[2\left(\frac{m_p}{m_n}\right)^{3/4}\sqrt{\frac{c_p}{c_n}}\right]. \quad (11)$$

In order to divide the reduced recombination rate into components corresponding to the recombination flows through separate recombination centers, the following notation was introduced:

$$\alpha_m = (n_{1m}/n_i)\, c_{nm} N_{tm},\ \zeta_m = (n_{1m}/n_i)\, (c_{nm}/c_{pm})^{1/2}$$

(here the equality $n_{1m}p_{1m} = n_i^2$ is used), then

$$R_{np}(U) = \sum_{m=1}^{g} \frac{\alpha_m \exp\left(\frac{qU}{2kT}\right)}{2\zeta_m \exp\left(\frac{qU}{2kT}\right) + \zeta_m^2 + 1}. \quad (12)$$

Each term in (12) corresponds to a recombination center with number m and is described by two parameters α_m and ζ_m. It is possible to determine the pre-exponential factor $\alpha_m/(\zeta_m^2 + 1)$ in (12) from the initial segment, and $\alpha_m/(2\zeta_m)$ from the final segment, after which we can find α_m and ζ_m, which, in turn, are related to deep level parameters,[21–23]

$$E_{tn\,m} = \frac{E_g}{2} - kT \ln \zeta_m + \frac{3}{4} kT \ln \frac{m_n^*}{m_p^*} + \frac{1}{2} kT \ln \frac{c_n}{c_p}, \quad (13)$$

where E_g is the semiconductor bandgap, m_n^* and m_p^* are the effective masses of electrons and holes, respectively, $E_{tn\,m} = E_C - E_{t\,m}$, $E_{tp\,m} = E_{t\,m} - E_V$.

Estimation of the lifetime can be done by the formula,

$$\sqrt{\tau_{n0}\,\tau_{p0}} = \left(\frac{1}{c_n N_t}\right)^{1/2} \times \left(\frac{1}{c_p N_t}\right)^{1/2} = \frac{\zeta}{\alpha}, \quad (14)$$

where τ_{n0} is the lifetime during capture of an electron to a level filled with holes and τ_{p0} is the lifetime during capture of a hole to a level filled with electrons.

To separate $R_{np}(U)$ into components and find the values α_m and ζ_m, it is convenient to use regression analysis when the experimental curve $R_{np}(U)$ is approximated by the theoretical model dependence (12) and compared with the experiment. It turns out a set of values of the parameters α_m and ζ_m (m = 1,…,g) as a result of optimization of the standard deviation of the experiment from approximation.

For the calculation of $R_{np}(U)$ by formula (7), the capacitance–voltage characteristic was previously measured, from which V_d and dependence $w(U)$ were determined. The experimental dependences of the reduced recombination rate of each of the studied samples were divided into three recombination processes (see Fig. 8); α and ζ were determined for each of them at different temperatures. The activation energy E_{tn} and $\sqrt{\tau_{n0}\,\tau_{p0}}$ were calculated by formulas (13) and (14).

The reduced recombination rate is divided into three processes both before and after irradiation. Processes 1 and 2 in Figs. 8(a) and 8(b) remain almost identical. Process 3 are different. Before irradiation, the reduced saturation recombination rate is lower than after irradiation. This is natural, because irradiation introduces additional centers and this value grows in accordance with formula (10). However, the inflection voltage (U_{inf}) changes, which is greater before irradiation than after irradiation. This means that after irradiation, the energy of the recombination center also became approximately 0.1 eV higher, as follows from formula (11). Apparently, irradiation leads to the appearance of another recombination center, which takes precedence over the previous one.

Lifetimes were calculated using formula (14), which are shown in Fig. 9(a). They exhibit a strong temperature dependence. The same dependencies plotted in the Arrhenius coordinates [see Fig. 9(b)] have extended linear sections. This indicates that the lifetime at high temperatures varies exponentially like $\exp(-\Delta E/kT)$. An exponential change in the lifetime indicates that in order to capture an electron or hole at a given recombination center, it is necessary to overcome a potential barrier with energy ΔE. This energy is 0.46 eV before irradiation and 0.17 eV after irradiation.

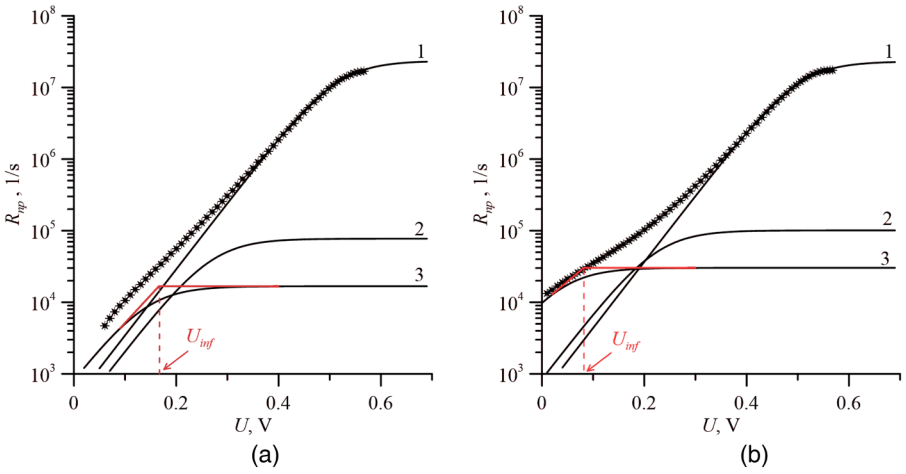

FIG. 8. Separation of $R_{np}(U)$ into components at a temperature of 0 °C: (a) before irradiation; (b) after irradiation. Curves 1–3 are the recombination processes associated with various recombination centers that have deep levels in the bandgap of silicon.

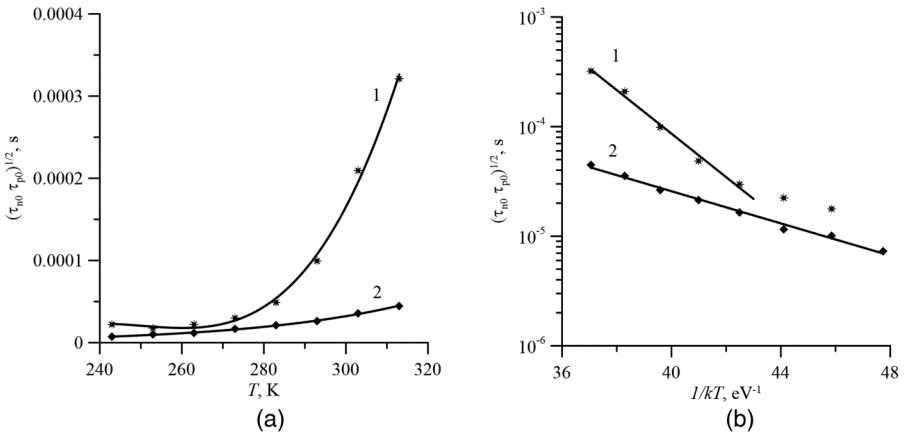

FIG. 9. Temperature dependences of the lifetime for the recombination process 3: 1—before irradiation, 2—after irradiation.

The temperature dependences of the lifetime (see Fig. 9) and the capture energy at the recombination center are different, which also indicates that a new recombination center appears upon irradiation.

The activation energies of recombination centers before and after irradiation are shown in Table II. The energy of the deep level of recombination centers that determine process 3 before irradiation is 0.47 eV and after irradiation is 0.54 eV. Therefore, irradiation introduces a new recombination center.

Analysis of publications on defects in silicon shows that the activation energy of 0.47 eV can correspond to a complex of a silicon vacancy with oxygen (V–O)[2,14,36] or divacancy.[2,9,12,14] Recombination centers with an activation energy of 0.54 eV are associated with a complex of two vacancies with oxygen (V_2–O).[16,17] It can be assumed that upon irradiation, when the concentration of silicon vacancies increases, a reaction takes place in a solid of the type V–O + V → V_2–O. The possibility of such transformations is indicated by the results of Refs. 18 and 19.

III. THE EFFECT OF ELECTRON–PHONON INTERACTION ON THE REVERSE CVC OF P–N JUNCTIONS WITH VACANCY-OXYGEN COMPLEXES

At reverse voltage, the SCR of the p–n junction is depleted in free charge carriers; the equilibrium between recombination and generation is shifted toward generation. The reverse current is determined by the expression,

$$I_{rev} = qA\int_0^w R dx, \tag{15}$$

where R is the generation rate. In the case of generation with the participation of the recombination center (RC), which has one deep level in the bandgap of the semiconductor, its rate can be found from the system of kinetic equations,

$$\begin{aligned} R_n &= \frac{dn}{dt} = -c_n n(N_t - n_t) + e_n^t n_t, \\ R_p &= \frac{dp}{dt} = -c_p p n_t + e_p^t (N_t - n_t), \end{aligned} \tag{16}$$

where N_t, e_n^t, e_p^t, c_n, c_p are previously defined, n_t is the concentration of electrons on RC.

When calculating the generation rate, it is taken into account that in the equilibrium position $R = R_n = R_p$ holds true. Using this equation, as well as the conditions $n = 0$ and $p = 0$ under reverse bias, substitution of system (16) in Eq. (15) gives,

$$I_{rev} = qA\int_0^w \frac{e_n^t(x) e_p^t(x) N_t(x)}{e_n^t(x) + e_p^t(x)} dx, \tag{17}$$

where $e_n^t = \gamma_n c_n N_c \exp(-(E_C - E_t)/kT)$, $e_p^t = \gamma_p c_p N_v \exp(-(E_t - E_V)/kT)$, and γ_n and γ_p are the degeneration factors of the deep center level for electrons and holes. These factors vary from 0.5 to 2.

It should be noted that the rate of thermal emission depends on the temperature exponentially; therefore, if the RC level differs from the middle of the bandgap by (3–5) kT; then, as a rule, the rate of emission of electrons or holes is much higher than the rate of another transition. We make the following approximations: the recombination level is located closer to the conduction band; RCs

TABLE II. Energies of deep levels of recombination centers at 0 °C.

Recombination process number as shown in Fig. 8	1	2	3
Energy before irradiation (eV)	0.27 ± 0.02	0.44 ± 0.02	0.47 ± 0.02
Energy after irradiation (eV)	0.27 ± 0.02	0.44 ± 0.02	0.54 ± 0.02

TABLE III. Parameters of generation centers, which determine the reverse current before and after irradiation. Note: The RC energy $E_t(0)$ was calculated using formula (19). For silicon, $E_g(0) \approx 1.17$ eV. The values of the parameters $S\hbar\omega$ and E_0were calculated from the joint solution of Eqs. (23) and (25). The values β_{Fex}, $E_{gen}(0)$, ΔE were found from the experiment.

Experimental and calculated parameters	β_{Fex} (eV × cm$^{1/2}$/V$^{1/2}$)	$E_{gen}(0)$ (eV)	$E_t(0)$ (eV)	$S\hbar\omega$ (eV)	E_0 (eV)	ΔE (eV)
Before irradiation	21.5×10^{-4}	0.85	0.32	0.003	0.063	0.46
After irradiation	7.4×10^{-4}	0.67	0.50	0.045	0.254	0.17

are evenly spaced across the SCR; thermal emission rates are independent of the electric field. It turns out a simple expression for the reverse current of the diode,

$$I_{rev} = qAw(U)N_t e_p^t. \tag{18}$$

Formula (18) includes the emission rate of holes, not electrons, since the magnitude of the current at reverse bias is determined by the slowest process, namely, the emission rate with higher activation energy. Therefore, in the case of thermal generation through the RC, the energy experimentally obtained is more than half the bandgap. Accordingly, the energy of the recombination center at zero electric field strength ($E_t(0)$) is related to the activation energy of the generation process (E_{gen}) by the expression,

$$E_t(0) = E_g(0) - E_{gen}(0). \tag{19}$$

Formula (18) shows that the generation current at reverse bias is directly proportional to the concentration of recombination centers and has voltage dependence, however weak. Therefore, it grows after irradiation. Formula (18), as a first approximation, correctly describes the temperature dependence of the current (see Fig. 2); however, this formula gives a dependence of the current on the reverse bias voltage by square or cubic root, which is due to a change in the width of the depletion region, and it does not follow that the activation energy of hole emission depends on the voltage. The experimentally measured current (see Fig. 2) varies exponentially from the reverse bias voltage, which is due to a change in the probability of emission depending on the electric field strength in the SCR of the p–n junction.

Lowering the height of the potential barrier due to the Pool–Frenkel effect[1] has the form,

$$\Delta E_t = \frac{q^{3/2}}{\sqrt{\pi\varepsilon\varepsilon_0}}\sqrt{F} = \beta_F\sqrt{F}. \tag{20}$$

The factor in front of the root of the electric field, which is called the Frenkel constant $\left(\beta_F = q^{3/2}/\sqrt{\pi\varepsilon\varepsilon_0}\right)$, does not depend on the technological parameters of the device, but is determined only by constants. Its value is in practical units 0.00 023 eV × cm$^{1/2}$/V$^{1/2}$.

With the help of formula (20), the expression for the CVC of the p–n junction at reverse bias is calculated,

$$\begin{aligned} I_{rev} &= qAe_{p0}^t \int_0^w N_t(x)\exp\left(\frac{\Delta E_t(x)}{kT}\right)dx \\ &= qAe_{p0}^t \int_0^w N_t(x)\exp\left(\frac{\beta_F\sqrt{F(x)}}{kT}\right)dx, \end{aligned} \tag{21}$$

where e_{p0}^t is the hole emission rate without taking into account the influence of the electric field.

Formula (21) takes into account the effect of both temperature and electric field strength. The energy of the generation process taking into account the Poole–Frenkel effect is

$$E_{gen}(F) = E_{gen}(0) - \beta_F\sqrt{F}, \tag{22}$$

where $E_{gen}(0)$ is the energy of the generation process in the absence of an electric field.

This dependence in coordinates $E_{gen}(F) = f(F^{1/2})$ looks like a straight line. The approximation of the experimental results in Fig. 4 has the same form, which makes it possible to determine the energy of the generation process in the absence of an electric field ($E_{gen}(0)$) and the experimental value of the Frenkel constant (β_{Fex}). These parameters are shown in Table III. The electron–phonon interaction leads to the fact that the defect must be characterized by several parameters and not by one activation energy.

In our case, the experimental values β_{Fex} are several times higher than the theoretical ones, which is associated with the electron–phonon interaction. In the work by Timashev, it is shown[34] that

$$\beta_{Fex} = \beta_F\left(1 + \frac{E_0 - S\hbar\omega}{2S\hbar\omega}\right), \tag{23}$$

where $S\hbar\omega$ is a value equal to half the heat release that accompanies the electron–phonon interaction; E_0 is the energy of a purely electronic transition, S is the Huang–Rhys factor, and $\hbar\omega$ is the energy of a characteristic phonon in the one-coordinate model.

Expression (23) is valid when the generation of charge carriers occurs as a result of a multiphonon process and only one type of phonons with some effective energy takes part in it. Such a model is called the one-coordinate model and for it one can use the configuration-coordinate diagram,[37,38] which is shown in Fig. 10

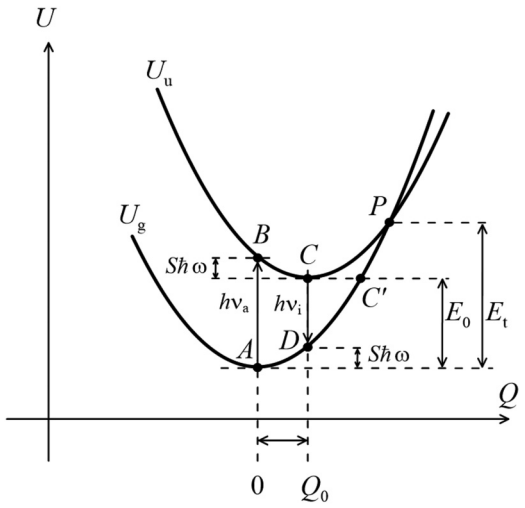

FIG. 10. Configuration-coordinate diagram.

and explains the meaning of the parameters of the electron–phonon interaction given in Table III.

The construction of such a diagram is based on a simplified approximation of the one-coordinate model, according to which the ground and excited states of the centers are described by adiabatic potentials, the energy of which is proportional to the square of a certain generalized coordinate Q. When the system passes from the ground state to the excited one, the polaron effect takes place, as a result of which the adiabatic potential of the excited state is shifted relative to the main potential by the amount Q_0 (polaron shift) and they intersect at point P (see Fig. 10),

$$U_g = \frac{\hbar\omega\, Q^2}{2}; \qquad U_u = \frac{\hbar\omega\,(Q - Q_0)^2}{2} + E_0, \tag{24}$$

where $Q_0 = \sqrt{2S}$, U_g is the adiabatic potential of the ground state of a center, U_u is the adiabatic potential of the excited state of a center, $h\nu_a$ is the energy of the absorption maximum during the transition from the ground state to the excited state, $h\nu_i$ is the energy of the maximum radiation during the transition from the excited state to the ground state, and E_t is the energy of thermal activation.

This model is used to describe the possibility of multiphonon non-radiative transitions of charge carriers and avoids the difficulties of explaining the simultaneous interaction of many particles. With a non-radiative transition from the ground state (point A in Fig. 10) to an excited one (point C, Fig. 10), the system absorbs one phonon after another while increasing the amplitude of the generalized coordinate. The transition itself occurs at the saddle point (point P, Fig. 10), when the energy of the ground state takes on the value E_t, and then the system relaxes to point C, also emitting phonons one after another to reduce the energy. In accordance with the approximation of the one-coordinate model for the electron–phonon interaction, the thermal generation energy is[37]

$$E_t(0) = \frac{(E_0 + S\hbar\omega)^2}{4S\hbar\omega}. \tag{25}$$

Formulas (23) and (25) allow calculating the parameters of the electron–phonon interaction $S\hbar\omega$ and E_0. These parameters are given in Table II. The value of the experimental Frenkel constant and the thermal activation energy of the generation process in the absence of an electric field $E_t(0)$ are calculated from the experimental data shown in Fig. 4. The results of calculations are presented in Table III. These parameters, as well as the energy of thermal activation $E_t(0)$, after irradiation take on different values (Table III).

The data given in Table III allow us to construct the configuration-coordinate diagrams of the centers, which determine the magnitude of the reverse currents of the p–n junction before and after irradiation. They are shown in Fig. 11.

These diagrams differ in the energies of purely electronic transitions and in the polaron shift, which also indicates a change in the nature of the recombination center after irradiation. The activation energies ΔE for the capture of charge carriers by the recombination center in the classical one-coordinate model and at high temperatures are related to the thermal activation energy $E_t(0)$ and the purely electronic transition energy E_0: $\Delta E = E_t(0) - E_0$. At

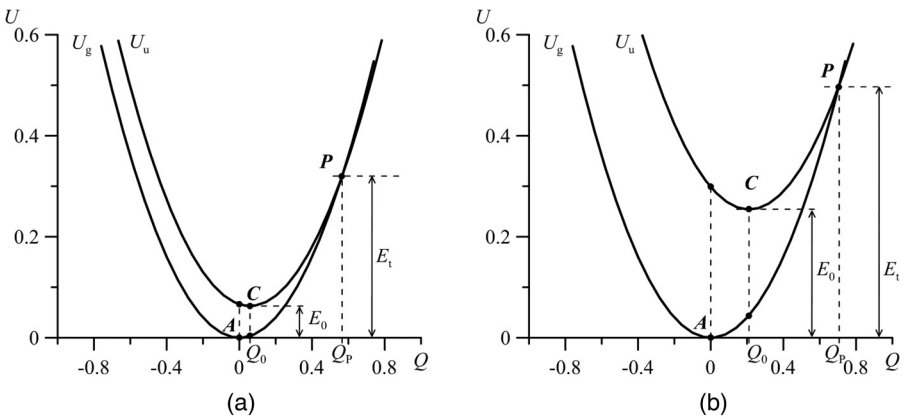

FIG. 11. Configuration-coordinate diagrams of recombination centers: (a) before irradiation; (b) after irradiation.

lower temperatures, the energy ΔE decreases because capture occurs by a tunneling method, rather than activation through a barrier with a maximum at point P. In our case, ΔE agrees with the difference between the thermal activation energy of the RC and the energy of a purely electronic transition.

The polaron shift (Q_0) and the activation energies of capture to the recombination center differ before and after irradiation. The polaron shift before irradiation is smaller, and the capture energy is higher than after irradiation, which indicates that the electron–phonon interaction is less pronounced before irradiation. The electron–phonon interaction, as a rule, manifests itself more strongly in molecular objects; therefore, it can be assumed that the nature of the recombination centers found in this work is associated with molecular complexes of a silicon vacancy with an impurity and is consistent with the conclusions of Sec. II, according to which, after irradiation, the V_2O center appears. It is known that at high irradiation doses in silicon diodes, there are processes associated with the metastability of such centers and with the Jahn–Teller effect, which are inherent in them,[36,39] which is also a manifestation of the electron–phonon interaction.

Two remarks should be made: first, local states near half the bandgap are involved in current generation. This is due to the fact that the generation rate decreases exponentially with an increase in the activation energy of the process. Second, the molecular centers of silicon are multiply charged and the manifestation of a different charge state depends on the conditions under which the measurement process takes place. When measuring the parameters of recombination centers by the method of deep level transient spectroscopy (DLTS), at each measurement event, the recombination centers are filled by applying a voltage to the diode in the forward direction. In this case, the parameters of the electronic state are measured, which have time to change their charge in a time equal to the width of the rates window in the DLTS experiment. Therefore, comparison with these experiments should be made with peaks located in the high-temperature region of DLTS. Note also that it is difficult to judge from capacitive experiments whether the center is doubly or multiply charged.

The experimental results of measuring the reverse currents agree with the analysis of the recombination currents, which show that irradiation results in the formation of centers of two silicon vacancies with oxygen, which also determine the magnitude of the reverse currents of diodes.[17–19] In this case, the generation of charge carriers is influenced by the electron–phonon interaction. We have developed a technique for determining the parameters of this interaction from the reverse CVC.

IV. CONCLUSION

An analysis of the experimental CVC of diodes shows that the current in them is determined by generation–recombination processes with the participation of recombination centers, which create deep levels in the semiconductor bandgap. The concentration of these recombination centers increases when the samples are irradiated with γ quanta. This leads to an increase in the recombination current due to a decrease in the lifetime. It is shown in this work that irradiation changes the ratio of various recombination centers in the SCR of the p–n junction. Since irradiation with γ quanta produces intrinsic point defects, including vacancies, it can be concluded that the observed recombination centers are associated with these defects and are complexes that arose as a result of the interaction of point intrinsic silicon defects with impurity atoms. The experimental results of this work, in comparison with the results of the work of other authors, show that, upon irradiation, centers of divacancy of silicon with oxygen are formed, which determine the magnitude of the reverse currents of the diodes. In this case, the generation of charge carriers is influenced by the electron–phonon interaction. We have developed a technique for determining the parameters of this interaction from the reverse CVC.

Application of the electron–phonon interaction model for analyzing the processes of recombination and generation in semiconductor diodes shows that it is not enough to characterize a recombination center with one deep level in the bandgap by only one activation energy. Such a center is characterized by the energy of capture of electrons and holes at the center, and energies of a purely electronic transition, heat release, and a polaron shift. All these parameters for the centers that determine the lifetime are given in Table III.

The CVCs, which were measured at forward bias, make it possible to calculate the activation energies of recombination centers and the lifetime of minority charge carriers at forward bias and in the temperature range −30 to +60 °C. So, one can be able to use the method of converting the CVC for express analysis of the quality of technological processes, when the parameters of the recombination centers are measured immediately on the plate, even when it is not cut into separate devices. This allows early diagnostics of power and optoelectronic devices immediately after the completion of the main technological processes.

ACKNOWLEDGMENTS

This work was supported by the Ministry of Science and Higher Education of the Russian Federation (Project No. 0004-2019-0001).

DATA AVAILABILITY

The data that support the findings of this study are available from the corresponding author upon reasonable request.

REFERENCES

[1]S. V. Bulyarskiy, "The effect of electron-phonon interaction on the formation of reverse currents of p-n-junctions of silicon-based power semiconductor devices," Solid-State Electron. **160**, 107624 (2019).
[2]S. Selberherr and P. Pichler, *Intrinsic Point Defects, Impurities, and Their Diffusion in Silicon* (Springer, Vienna, 2004).
[3]Y. V. Gorelkinskii, K. A. Abdullin, B. N. Mukashev, and T. S. Turmagambetov, "Self-interstitials and related defects in irradiated silicon," Physica B **404**, 4579–4582 (2009).
[4]P. Wang, C. Cui, X. Yu, and D. Yang, "Growth and ripening of oxygen precipitation in neutron-irradiated czochralski silicon," Mater. Sci. Semicond. Process. **74**, 369–374 (2018).
[5]Y. Qin, P. Wang, S. Jin, C. Cui, D. Yang, and X. Yu, "Effects of nitrogen doping on vacancy-oxygen complexes in neutron irradiated czochralski silicon," Mater. Sci. Semicond. Process. **98**, 65–69 (2019).

[6]S. J. Moloi and M. McPherson, "Reverse annealing studies of irradiated silicon by use of current–voltage measurements," Nucl. Instrum. Methods Phys. Res. Sect. B **440**, 64–67 (2019).
[7]X. Lu, Y. Song, J. Gao, X. Wang, and Y. Zhang, "The influences of the properties of impurities and defects on the dark I–V characteristic curve and output parameters of c-Si solar cells," Physica B **520**, 28–36 (2017).
[8]O. Y. Olikh, "Relationship between the ideality factor and the iron concentration in silicon solar cells," Superlattices Microstruct. **136**, 106309 (2019).
[9]A. M. Frens, M. T. Bennebroek, A. Zakrzewski, J. Schmidt, W. M. Chen, E. Janzén, J. L. Lindström, and B. Monemar, "Observation of rapid direct charge transfer between deep defects in silicon," Phys. Rev. Lett. **72**, 2939–2942 (1994).
[10]L. I. Murin, V. A. Gurinovich, I. F. Medvedeva, and V. P. Markevich, "Thermally stable carbon–oxygen complexes in irradiated silicon crystals," Inorg. Mater. Appl. Res. **7**, 192–195 (2016).
[11]G. P. Gaidar, "Annealing of radiation-induced defects in silicon," Surf. Eng. Appl. Electrochem. **48**, 78–89 (2012).
[12]J. H. Evans-Freeman, A. R. Peaker, I. D. Hawkins, P. Y. Y. Kan, J. Terry, L. Rubaldo, M. Ahmed, S. Watts, and L. Dobaczewski, "High-resolution DLTS studies of vacancy-related defects in irradiated and in ion-implanted n-type silicon," Mater. Sci. Semicond. Process. **3**, 237–241 (2000).
[13]I. Capan, Ž Pastuović, R. Siegele, and R. Jaćimović, "Vacancy-related defects in n -type Si implanted with a rarefied microbeam of accelerated heavy ions in the MeV range," Nucl. Instrum. Methods Phys. Res. Sect. B **372**, 156–160 (2016).
[14]P. Hazdra and V. Komarnitskyy, "Influence of radiation defects on formation of thermal donors in silicon irradiated with high-energy helium ions," Mater. Sci. Eng. B **159-160**, 346–349 (2009).
[15]G.-F. Chen, Y.-X. Li, L.-L. Liu, P.-J. Niu, S.-L. Niu, and D.-F. Chen, "Annealing behaviors of vacancy in varied neutron irradiated czochralski silicon," Trans. Nonferrous Met. Soc. China **16**, s113–s115 (2006).
[16]G. Alfieri, E. V. Monakhov, B. S. Avset, and B. G. Svensson, "Evidence for identification of the divacancy-oxygen center in Si," Phys. Rev. B **68**, 2653 (2003).
[17]M. Mikelsen, E. V. Monakhov, G. Alfieri, B. S. Avset, and B. G. Svensson, "Kinetics of divacancy annealing and divacancy-oxygen formation in oxygen-enriched high-purity silicon," Phys. Rev. B **72**, 523 (2005).
[18]J. L. Lindström, L. I. Murin, B. G. Svensson, V. P. Markevich, and T. Hallberg, "The VO_2* defect in silicon," Phys. B **340-342**, 509–513 (2003).
[19]A. Junkes, I. Pintilie, E. Fretwurst, and D. Eckstein, "A contribution to the identification of the E5 defect level as tri-vacancy (V3)," Phys. B **407**, 3013–3015 (2012).
[20]S. V. Bulyarskii, N. S. Grushko, A. I. Somov, and A. V. Lakalin, "Recombination in the space charge region and its effect on the transmittance of bipolar transistors," Semiconductors **31**, 983–987 (1997).
[21]S. V. Bulyarskii, N. S. Grushko, and A. V. Lakalin, "Differential methods for determination of deep-level parameters from recombination currents of p-n junctions," Semiconductors **32**, 1065–1068 (1998).
[22]S. V. Bulyarskii, M. O. Vorob'ev, N. S. Grushko, and A. V. Lakalin, "Determination of the parameters of deep levels using the differential coefficients of the current-voltage characteristics," Tech. Phys. Lett. **25**, 176–178 (1999).
[23]S. V. Bulyarskiy, A. V. Lakalin, I. E. Abanin, V. V. Amelichev, and V. V. Svetuhin, "Optimization of the parameters of power sources excited by β-radiation," Semiconductors **51**, 66–72 (2017).
[24]W. Shockley, "The theory of p–n junctions in semiconductors and p–n junction transistors," Bell Syst. Tech. J. **28**, 435–489 (1949).
[25]C.-T. Sah, R. Noyce, and W. Shockley, "Carrier generation and recombination in p–n junctions and p–n junction characteristics," Proc. IRE **45**, 1228–1243 (1957).
[26]S. Rein, T. Rehrl, W. Warta, and S. W. Glunz, "Lifetime spectroscopy for defect characterization: Systematic analysis of the possibilities and restrictions," J. Appl. Phys. **91**, 2059–2070 (2002).
[27]E. Simoen, C. Claeys, and J. Vanhellemont, "Defect analysis in semiconductor materials based on p–n junction diode characteristics," Defect Diffus. Forum **261–262**, 1–24 (2007).
[28]E. Simoen and C. Claeys, "On the impact of the capture rates on the generation/recombination lifetime ratio of a single deep level," IEEE Trans. Electron Devices **46**, 1487–1488 (1999).
[29]D. Macdonald and A. Cuevas, "Validity of simplified Shockley–Read–Hall statistics for modeling carrier lifetimes in crystalline silicon," Phys. Rev. B **67**, 2059 (2003).
[30]B. Biro, G. David, A. Fenyvesi, J. S. Haggerty, J. Kierstead, E. J. Mannel, T. Majoros, J. Molnar, F. Nagy, S. Stoll, B. Ujvari, and C. L. Woody, "A comparison of the effects of neutron and gamma radiation in silicon photomultipliers," IEEE Trans. Nucl. Sci. **66**, 1833–1839 (2019).
[31]K. A. Abdullah, F. A. Alloush, A. Jaafar, and C. Salame, "Study of the effects related to the electric reverse stress currents on the mono-Si solar cell electrical parameters," Energy Procedia **36**, 104–113 (2013).
[32]Q. Shan, D. S. Meyaard, Q. Dai, J. Cho, E. Fred Schubert, J. Kon Son, and C. Sone, "Transport-mechanism analysis of the reverse leakage current in GaInN light-emitting diodes," Appl. Phys. Lett. **99**, 253506 (2011).
[33]M. Musolino, D. van Treeck, A. Tahraoui, L. Scarparo, C. de Santi, M. Meneghini, E. Zanoni, L. Geelhaar, and H. Riechert, "A physical model for the reverse leakage current in (In,Ga)N/GaN light-emitting diodes based on nanowires," J. Appl. Phys. **119**, 044502 (2016).
[34]S. F. Timashev, "Ob effekte Frenkelya pri termo-polevoj ionizacii glubokih centrov v oblasti prostranstvennogo zaryada v poluprovodnikah [On the Frenkel effect during thermo-field ionization of deep centers in the space charge layer in semiconductors] (in Russian)," Fiz. Tekh. Poluprovodn. **8**, 804–806 (1974).
[35]V. V. N. Obreja, "On the leakage current of present-day manufactured semiconductor junctions," Solid-State Electron. **44**, 49–57 (2000).
[36]S. B. Lastovskii, V. P. Markevich, H. S. Yakushevich, L. I. Murin, and V. P. Krylov, "Radiation-induced bistable centers with deep levels in silicon n+–p structures," Semiconductors **50**, 751–755 (2016).
[37]A. N. Saurov and S. V. Bulyarskiy, *Fizika Poluprovodnikovyh Preobrazovatelej [Physics of Semiconductor Converters] (in Russian)* (Russian Academy of Sciences, Moscow, 2018).
[38]B. K. Ridley, *Quantum Processes in Semiconductors*, 3rd ed. (Oxford University Press, Oxford, 1993).
[39]L. I. Murin, V. P. Markevich, I. F. Medvedeva, and L. Dobaczewski, "Bistability and electrical activity of the vacancy–dioxygen complex in silicon," Semiconductors **40**, 1282–1286 (2006).